First and Second Law Analysis for the MHD Flow of Two Immiscible Couple Stress Fluids between Two Parallel Plates

Data · June 2015

CITATIONS
2

READS
234

2 authors:

Ramana Murthy Josyula
National Institute of Technology, Warangal
71 PUBLICATIONS **849** CITATIONS
SEE PROFILE

Srinivas Jangili
National Institute of Technology, Warangal
34 PUBLICATIONS **673** CITATIONS
SEE PROFILE

Heat Transfer—Asian Research, **44** (5), 2015

First and Second Law Analysis for the MHD Flow of Two Immiscible Couple Stress Fluids between Two Parallel Plates

J. V. Ramana Murthy and J. Srinivas
Department of Mathematics, National Institute of Technology, Warangal, 506004, AP, India

This paper aims to analyze the heat transfer by the first and second laws of thermodynamics for the flow of two immiscible couple stress fluids inside a horizontal channel under the action of an imposed transverse magnetic field. The plates of the channel are maintained at constant and different temperatures higher than that of the fluid. The flow region consists of two zones, the flow of the heavier fluid taking place in the lower zone. No slip condition is taken on the plates and continuity of velocity, vorticity, shear stress, couple stress, temperature, and heat flux are imposed at the interface. The velocity and temperature distributions are derived analytically and these are used to compute the dimensionless expressions for the entropy generation number and Bejan number. The results are presented graphically. It is observed that the imposed magnetic field reduces the entropy production rate near the plates. Heat Trans Asian Res, 44(5): 468–487, 2015; Published online in Wiley Online Library (wileyonlinelibrary.com/journal/htj). DOI 10.1002/htj.21131

Key words: immiscible fluids, couple stress fluid, MHD, entropy generation number, Bejan number

1. Introduction

During the past few decades, in thermodynamic analysis, especially, the second law analysis has been appearing to be an essential tool for the design and optimization of thermal systems. The second law analysis is one of the best tools for improving the performance of thermal systems involving heat transfer. It examines the irreversibility due to fluid flow and heat transfer in terms of the entropy generation rate. Entropy generation is used in thermodynamics as a criterion to quantify the significance of irreversibilities. The second law of thermodynamics provides a general and unique way of optimizing the design of thermal-fluid devices both thermally and hydrodynamically by minimizing the sum of thermal and frictional entropy generation rates. This process of minimization is popularly known as the entropy generation minimization (EGM) method. Further, it can be used to predict the performance of a thermal system in engineering processes. Thus in entropy generation analysis, a set of optimal operating and design conditions are obtained that minimize the irreversibilities in the system. Accurate estimation of the entropy generation rate plays an important role in the design and development of thermo fluid components such as heat exchangers, energy storage systems, pumps, turbines, electronic cooling devices, and so on. The different effective factors

behind entropy generation in a thermal process/system, where the destruction of available energy of a system occurs during the generation of entropy, have been investigated by Bejan [1, 2].

In thermodynamics, exergy is defined as the maximum amount of work which can be produced by a system or a flow of matter or energy as it comes to equilibrium with a reference environment. Unlike energy, exergy is not subjected to a conservation law. Exergy is consumed or destroyed, due to irreversibility's in any real process. Second law (exergy analysis) quantifies and locates the losses that help in optimizing the thermal systems. Second law analysis helps us in evaluating inefficiencies associated with the various processes. The heat transfer process in any system involves exergy losses or loss of the available work due to temperature gradients and fluid frictions and this is due to the irreversible work involved in the process. The exergy loss is proportional to the entropy generation rate [1]. Hence minimization of the entropy generation rate indicates optimum exergy or the amount of available work. The study of entropy production or second law analysis of thermodynamics is the gateway for optimization studies in thermal equipment and systems. This new approach is important and, at the same time, necessary, to increase viable engineering solutions to energy problems. The new methodology is called exergy analysis. The analysis of energy utilization and entropy generation is one of the primary objectives in designing a thermal system. The entropy generation and its minimization were investigated extensively by Bejan [2–4], who presented systematically the concept and working procedure. Bejan [5, 6] studied the heat transfer problems in pipe flow, boundary layer flow past a plate, and flow in the entrance region of a rectangular duct using EGM. He showed that engineering design of a thermal system could be improved through minimizing the entropy generation. San and colleagues [7] were the first to have an analytical study of the effect of mass transfer on entropy generation in forced convection between two parallel plates. They have shown that under the criteria $(\frac{L}{4r_h}) \gg 0.05\mathrm{Re}\,\mathrm{Pr}$, the flow is fully developed and the optimum spacing between the plates can be obtained by the equation of mean fluid temperature distribution. Later on, many investigations have been carried to determine the entropy generation and Bejan profiles for different geometric arrangements, flow situations, and thermal boundary conditions. Demirel and Kahraman [8] made a thermodynamic analysis for an annular packed bed with asymmetric heating. Delavar and Hedayatpour [9] have investigated the entropy generation characteristics in a channel with a heat-generating porous block using the lattice Boltzmann method and found that the entropy generation rate is more in a porous block compared to that of a clear fluid block. Kamel Hooman and colleagues [10] observed that near the entrance region the entire heat lines changes their direction suddenly in a narrow region for a thermally developing fluid flow in saturated porous medium between two plates.

There are many problems in the fields of hydrology and reservoir mechanics in which systems involving two or more immiscible fluids of different densities/viscosities flowing in the same pipe or channel or through porous media are encountered. Typical fluid examples of these systems are: air–water, water–salt water, oil–water, gas–oil, and gas–oil–water systems. These are referred to as multiphase flows in literature. Blood flow in arteries has been studied by many researchers considering blood as a two phase flow. Several investigations on multiphase flows are reported by various researchers such as Bird and colleagues [11], Chaturani and Ponnalagar Samy [12], Ramchandra Rao and Srinivasan Usha [13], and so on. The flow and heat transfer in immiscible fluids are of special importance in petroleum extraction and transport problems. Heat transfer in immiscible flows were discussed by Bakhtiyarov and Siginer [14], Prathap Kumar and colleagues [15], Chamkha [16], and so on.

In the last few decades, many studies have been developed in order to investigate the effect of a magnetic field on different geometries [17, 18]. Alpher [19] discussed the heat transfer in a magneto hydrodynamic flow between parallel plates. Nikodijevic and colleagues [20] studied the Couette two-fluid flow and heat transfer in the presence of a uniform inclined magnetic field. It is also to be noted that the analytical study of first and second laws of thermodynamics for the flow within a channel in the presence of a magnetic field is significant in many industrial applications, such as MHD marine propulsion, electronic packages, microelectronic devices, MHD generators, pumps, accelerators, filtration, geothermal systems, and have applications in nuclear reactors too. Some other quite promising applications are in the field of metallurgy such as MHD stirring of molten metal and magnetic-levitation casting. Several works have been reported on the effect of MHD flow on entropy generation for various flows and geometries by Damseh and colleagues [21], Mahian and colleagues [22], Kiyasatfar and colleagues [23], Chin-Chia Liu and Cheng-Ying Lo [24], and so on. In recent years, the fluid flow and entropy generation in two immiscible fluids in a channel have received considerable attention by researchers. Kamisli and Oztop [25] considered the fluid flow and entropy generation in two immiscible fluids in a channel. These authors explained the thermodynamic interface conditions involved in a flow of immiscible fluids and made a significant observation that minimum temperature gradient in the transverse direction of the flow offers minimum entropy generation near the plates.

To the extent the present authors have surveyed, the flow of immiscible incompressible couple stress fluids between two parallel plates has not been studied. The classical Navier–Stokes theory does not describe the flow properties of polymeric fluids, colloidal suspension and fluids containing certain additives. Different models have been proposed by many authors to explain the behavior of such fluids. Stokes [26] proposed the theory of couple stress fluids for fluids which have distinct features, such as the presence of couple stresses, body couples and nonsymmetric stress tensors. Their accurate flow behavior cannot be predicted by the classical Newtonian theory. The main effect of couple stresses is to introduce a size dependent effect that is not presented in the classical viscous fluid theory. The fluids consisting of rigid, randomly oriented particles suspended in a viscous medium, such as blood, lubricants containing small amount of polymer additives, electro-rheological fluids and synthetic fluids are all examples of these fluids. The couple stress fluid theory presents models for fluids whose microstructure is of mechanical significance. The effect of very small microstructure in a fluid can be felt if the characteristic geometric dimension of the problem considered is of the same order of magnitude as the size of the microstructure. Classical continuum mechanics neglects the size effect of material particles within the continua. However, in some important cases such as fluid flow with suspended particles, this cannot be true and a size dependent couple stress theory is needed. The spin field due to the rotation of freely suspended particles sets up an antisymmetric stress, known as couple-stress, leading thus to the couple stress fluid theory. These fluids are capable of describing various types of lubricants, blood, suspension fluids, and so on. The study of couple-stress fluids have applications in a number of processes that occur in various industries such as the extrusion of polymer fluids, solidification of liquid crystals, cooling of metallic plate in a bath, colloidal solutions, and so on. Stokes discussed the hydromagnetic steady flow of a fluid with couple stress effects. A review of couple stress (polar) fluid dynamics was reported by Stokes [27]. Soundalgekar [28] discussed the effects of couple stresses on MHD Couette flow. Application of the couple stress fluid model to biomechanics problems has been proposed in the study of peristaltic transport [29, 30]. Many authors have investigated the couple stress effects with reference to different lubrication problems [31–33].

The main objective of this study is to examine the entropy generation characteristics in a channel of two immiscible couple stress fluids under the influence of a transverse magnetic field.

Nomenclature

Be: Bejan number ($\frac{1}{1+\Phi}$)
Br: Brinkman number (=EkPr)
Br/Ω: viscous dissipation parameter
d_{ij}: components of the strain
D: deformation tensor
E: specific internal energy
Ek: Eckert number
$\bar{f}$: body forces per unit mass
$2h$: height of the free channel
Ha: Hartmann number
$\bar{\mathbf{h}}$: heat flux
k_1, k_2: thermal conductivity of the fluid in Zone I, II
$\bar{\ell}$: body couple per unit mass
M: couple stress tensor
n_η: couple stress coefficients ratio ($= \frac{\eta_2}{\eta_1}$)
n_k: thermal conductivity ratio ($= \frac{\mathrm{k_2}}{\mathrm{k_1}}$)
n_μ: viscosity ratio ($= \frac{\mu_2}{\mu_1}$)
n_σ: electric conductivity ratio ($= \frac{\rho_2}{\rho_1}$)
Nf: entropy generation due to viscous dissipation
Nm: entropy generation due to magnetic field
Ns: dimensionless total entropy generation number
Ny: entropy generation due to transverse conduction
Nu: Nusselt number
P: pressure
Pr: Prandtl number
$\bar{q}$: velocity vector
Re: Reynolds number
s_1, s_2: couple stress parameters
$(S_i)_G$: entropy generation rate
$(S_1)_{G,C}$: characteristic entropy transfer rate
τ: stress tensor
T_{I}, T_{II}: nondimensional temperatures of the plates
u: nondimensional velocity component in x-direction
x, y: nondimensional space coordinates
X, Y: space coordinates

Greek Symbols

η, η': couple stress viscosity coefficients

$\bar{\omega}$: rotation of the fluid particle
Ω: dimensionless temperature difference($= \frac{\Delta T}{T_o}$)
Φ: dissipation function
ϕ: irreversibility distribution ratio
ρ: density
θ: nondimensional temperature

Subscripts

1: fluid in Zone I
2: fluid in Zone II

2. Formulation of the Problem and Governing Equations

Consider the flow of two immiscible couple stress fluids between two parallel plates extending in the axial direction and distant $2h$ apart. Where X and Y are the axial and transverse coordinates respectively with the origin at the centre of the channel (Fig. 1). The length of the plates is much greater than the distance between them so that the flow at any point in the X-direction is the same. Fluid flow is generated due to a constant pressure gradient which acts at the mouth of the channel. A constant transverse magnetic field is applied on the plates. The fluid in the lower zone (viscosity μ_1, density ρ_1 and thermal conductivity k_1) occupies the region $(-h \leq Y \leq 0)$, comprising the lower half of the channel and this region is named Zone I. The fluid in the upper zone (viscosity μ_2, density $\rho_2 (< \rho_1)$ and thermal conductivity k_2) is assumed to occupy the upper half of the channel $(0 \leq Y \leq h)$, and this region is called Zone II. The two walls of the channel are held at different temperatures T_{I} and T_{II} (with $T_{\mathrm{I}} < T_{\mathrm{II}}$). The equations for the flow and energy in Zone I and II (i.e. $-h \leq \mathrm{Y} \leq \mathrm{h}$) are assumed to be governed by couple stress fluid flow equations as given by Stokes [26, 27]

$$\frac{\partial \rho}{\partial t} + \nabla.(\rho \bar{q}) = 0 \tag{1}$$

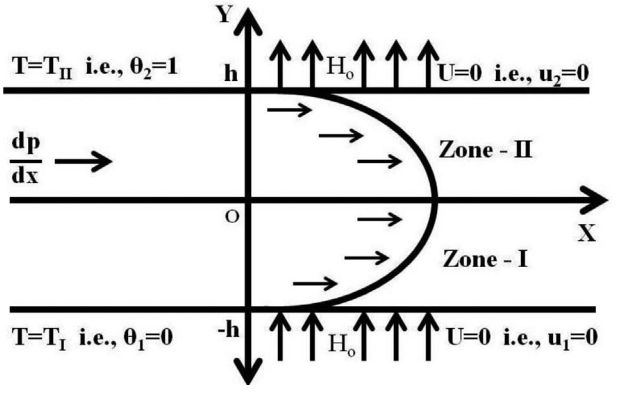

Fig. 1. Geometry of the problem.

$$\rho\left[\frac{d\bar{q}}{dt}+(\bar{q}.\nabla)\,\bar{q}\right]=-\nabla P+\mu\nabla\times\nabla\times\bar{q}-\eta\nabla\times\nabla\times\nabla\times\nabla\times\bar{q}+(\lambda+2\mu)\,\nabla\,(\nabla.\bar{q}) \tag{2}$$

$$\rho\frac{dE}{dt}=\Phi+k\nabla^2T+\frac{\bar{J}^2}{\sigma}, \tag{3}$$

where $\Phi=\mu[(\nabla\bar{q}):(\nabla\bar{q})^T+(\nabla\bar{q}):(\nabla\bar{q})]+4\eta[(\nabla\bar{\omega}):(\nabla\bar{\omega})^T]+4\eta'[(\nabla\bar{\omega}):(\nabla\bar{\omega})^T]$.

Equations (1)–(3) represent conservation of mass, balance of linear momentum and energy equation, respectively. The scalar quantity ρ is the density and P is the fluid pressure at any point. The vectors $\bar{q}$, $\bar{\omega}=\frac{1}{2}(\nabla\times\bar{q})$, $\bar{f}$, and $\bar{\ell}$ are velocity, rotation, body force per unit mass and body couple per unit mass, respectively. The material constants λ and μ are the viscosity coefficients and η and η' are the couple stress viscosity coefficients satisfying the constraints $\mu\geq 0$; $3\lambda+2\mu\geq 0$; $\eta\geq 0$; $|\eta'|\leq\eta$. There is a length parameter $l=\sqrt{\eta/\mu}$ which is a characteristic measure of the polarity of the couple stress fluid and this parameter is identically zero in the case of non-polar fluids. In the energy equation Φ is the dissipation function of mechanical energy per unit mass, E is the specific internal energy, $\bar{h}=-k\nabla T$ is the heat flux, where k is the thermal conductivity and T is the temperature. The current density $\bar{J}$, magnetic field $\bar{H}$ and electric field $\bar{E}$ are related by Maxwell's equations $\nabla\times\bar{E}=0$, $\nabla\times\bar{H}=\mu^1\bar{J}$, $\nabla\cdot\bar{J}=0$, $\bar{J}=\sigma(\bar{E}+\bar{q}\times\bar{H})$, where μ^1 is the magnetic permeability and σ is the electric conductivity.

To develop the governing equations for the problem considered, the following assumptions are made:

(i) The flow is assumed to be one-dimensional, incompressible, laminar, steady and fully developed.

(ii) The Lorentz force $\left(\bar{J}\times\bar{H}\right)$ is the only body force acting on the fluid.

(iii) The magnetic Reynolds number is assumed to be small, so that the induced magnetic field is neglected and the Hall effect of magneto hydrodynamics is assumed to be negligible.

It is assumed that the velocity of the fluid $\bar{q}=(U(Y),\,0,\,0)$, which satisfies the continuity Equation (1). The flow is subjected to a uniform applied magnetic field H_o in the positive y-direction, i.e., $\bar{H}=H_o\bar{j}$ which yields $\bar{J}\times\bar{H}=-\sigma H_o^2\bar{q}$. Under the assumptions made, the governing fluid flow Eq. (2) (in absence of body couple) of the problem is given by

$$\frac{\partial P}{\partial X}=\mu\frac{\partial^2U}{\partial Y^2}-\eta\frac{\partial^4U}{\partial Y^4}-\sigma H_o^2U. \tag{4}$$

The following nondimensional quantities are introduced to make the governing equations and the boundary conditions dimensionless: $x=\frac{X}{h}$, $y=\frac{Y}{h}$, $u=\frac{U}{U_o}$, $p=\frac{P}{\rho_1U_o^2}$, where U_o is the maximum velocity of the fluid in the channel.

Equation (4) in the corresponding zones in non-dimensional form is presented below: Zone I: $(-1\leq y\leq 0)$

The governing equation in Zone I is:

$$\frac{d^4u_1}{dy^4} - s_1\frac{d^2u_1}{dy^2} + Ha^2 s_1 u = -\mathrm{Re}\, s_1\frac{dp}{dx}. \tag{5}$$

Zone II: $(0 \le y \le 1)$

The governing equation in Zone II is:

$$\frac{d^4u_2}{dy^4} - s_2\frac{d^2u_2}{dy^2} + \frac{n_\sigma}{n_\mu}\mathrm{Ha}^2 s_2 u = -\frac{1}{n_\mu}\mathrm{Re}\, s_2\frac{dp}{dx}, \tag{6}$$

where $\mathrm{Re} = \frac{\rho_1 U_o h}{\mu_1}$ is the Reynolds number, $s_i = \frac{\mu_i h^2}{\gamma_i}$ is the couple stress parameter, $\mathrm{Ha}^2 = \frac{\sigma_1 H_o^2 h^2}{\mu_1}$. Hartmann number, $n_\sigma = \frac{\sigma_2}{\sigma_1}$ is the electric conductivity ratio and $n_\mu = \frac{\mu_2}{\mu_1}$ is the viscosity ratio $(i = 1, 2)$.

2.1 Boundary and interface conditions

A characteristic feature of a two-layer flow is the coupling across liquid–liquid interfaces. The liquid layers are mechanically coupled via transfer of momentum across the interfaces. Transfer of momentum results from the continuity of tangential velocity and a stress balance across the interface.

To determine the velocity components $u_1(y)$, $u_2(y)$ in Zones I and II described above, we adopt the following boundary and interface conditions:

Zone I is constituted by the fixed lower plate given by $y = -1$ and a fluid–fluid interface defined by $y = 0$. Zone II is constituted by the fluid interface given by $y = 0$ and the fixed upper plate given by $y = 1$.

In view of the no slip condition on the static boundaries, we have to prescribe

$$u_1 = 0 \quad \text{on} \quad y = -1 \quad \text{and} \quad u_2 = 0 \quad \text{on} \quad y = 1 \tag{7}$$

which represent the no slip condition.

Stokes [27] has proposed two types of boundary Conditions (A) and (B), respectively and the vanishing of couple stresses on the boundary is referred to as Condition (A). This condition is adopted here as this is appropriate in the present context. On the static boundary, this leads to

$$\frac{d^2u_1}{dy^2} = 0 \quad \text{at } y = -1 \quad \text{and} \quad \frac{d^2u_2}{dy^2} = 0 \quad \text{at } y = 1. \tag{8}$$

At the fluid–fluid interface $y = 0$, we assume that the velocity, vorticity, shear stress, and couple stress components are continuous. This implies

$$u_1(0^-) = u_2\left(0^+\right),\ \frac{du_1(0^-)}{dy} = \frac{du_2\left(0^+\right)}{dy},\ \tau_{xy}|_1(0^-) = \tau_{xy}|_2\left(0^+\right) \quad \text{and}$$
$$M_{xy}|_1(0^-) = M_{xy}|_2\left(0^+\right) \ \text{ at } \ y = 0. \tag{9}$$

The last two conditions of Eq. (9) give us

$$\left(s_1\frac{du_1}{dy}-\frac{d^3u_1}{dy^3}\right)_{y=0}=n_\eta\left(s_2\frac{du_2}{dy}-\frac{d^3u_2}{dy^3}\right)_{y=0},\ \left(\frac{d^2u_1}{dy^2}\right)_{y=0}=n_\eta\left(\frac{d^2u_2}{dy^2}\right)_{y=0}, \quad (10)$$

where $n_\eta=\frac{\eta_2}{\eta_1}$ is the couple stress coefficient ratio.

3. Solution of the Problem

3.1 Velocity distributions

Zone I: $(-1\le y\le 0)$

Solving Eqs. (5) and (6), we see that the velocity component of Zone I is given by

$$u_1(y)=c_{11}\,\mathrm{Cosh}\,\alpha_1 y+c_{12}\,\mathrm{Sinh}\,\alpha_1 y+c_{13}\,\mathrm{Cosh}\,\alpha_2 y+c_{14}\,\mathrm{Sinh}\,\alpha_2 y-\frac{1}{Ha^2}\mathrm{Re\,B} \quad (11)$$

Zone II: $(0\le y\le 1)$

and that of Zone II is given by

$$u_2(y)=c_{21}\,\mathrm{Cosh}\,\alpha_3 y+c_{22}\,\mathrm{Sinh}\,\alpha_3 y+c_{23}\,\mathrm{Cosh}\,\alpha_4 y+c_{24}\,\mathrm{Sinh}\,\alpha_4 y-\frac{1}{n_\sigma Ha^2}\mathrm{Re\,B}, \quad (12)$$

where α_1^2, α_2^2 are the roots of $x^2-a_1x+a_2=0$ and α_3^2, α_4^2 are the roots of $x^2-b_1x+b_2=0$ and $a_1=\alpha_1^2+\alpha_2^2=s_1$, $a_2=\alpha_1^2\alpha_2^2=Ha^2s_1$, $b_1=\alpha_3^2+\alpha_4^2=s_2$, $b_2=\alpha_3^2\alpha_4^2=(\frac{n_\sigma}{n_\mu})Ha^2s_2$.

The solutions $u_1(y)$ and $u_2(y)$ involve eight constants c_{11}, c_{12}, c_{13}, c_{14}, c_{21}, c_{22}, c_{23}, and c_{24}. These constants are found from the boundary conditions given in Eqs. (7)–(9) and are solved using Mathematica. As the expressions are cumbersome, they are not presented here.

3.2 Temperature distributions

Once the velocity distributions are known, the temperature distributions for the two zones are determined by solving the energy equation (3) in the respective zones, subject to the appropriate boundary and interface conditions. Thermal coupling is achieved through continuity of temperature at the interface and the balance of heat flux across the interface. In the present problem, it is assumed that the two plates are maintained at constant temperatures T_I and T_II $(T_\mathrm{I}<T_\mathrm{II})$.

We take temperature $T(Y)$ as,

$$T(Y)=\begin{cases}T_1(Y), & -h\le Y\le 0\\ T_2(Y), & 0\le Y\le h\end{cases}.$$

The governing equation for the temperature T_1 of the conducting fluid in Zone I is then given by

$$k_1 \frac{d^2 T_1}{dY^2} = -\left[\mu_1 \left(\frac{dU_1}{dY}\right)^2 + \eta_1 \left(\frac{d^2 U_1}{dY^2}\right)^2 + \sigma_1 H_o^2 U_1^2\right]. \tag{13}$$

The governing equation for the temperature T_2 of the conducting fluid in Zone II is then given by

$$k_2 \frac{d^2 T_2}{dY^2} = -\left[\mu_2 \left(\frac{dU_2}{dY}\right)^2 + \eta_2 \left(\frac{d^2 U_2}{dY^2}\right)^2 + \sigma_2 H_o^2 U_2^2\right]. \tag{14}$$

In order to nondimensionalize the above equations, the following transformation is used in addition to those already introduced in above: $\theta = \frac{T - T_I}{T_{II} - T_I}$.

Equations (13) and (14) are then reduced to the following form:

$$\frac{d^2\theta_1}{dy^2} = -Br\left[\left(\frac{du_1}{dy}\right)^2 + \frac{1}{s_1}\left(\frac{d^2 u_1}{dy^2}\right)^2 + Ha^2 u_1^2\right] \tag{15}$$

$$\frac{d^2\theta_2}{dy^2} = -\frac{Br\, n_\mu}{n_k}\left[\left(\frac{du_2}{dy}\right)^2 + \frac{1}{s_2}\left(\frac{d^2 u_2}{dy^2}\right)^2 + \frac{n_\sigma}{n_\mu} Ha^2 u_2^2\right], \tag{16}$$

where Br = Ek Pr is the Brinkman number, $Ek = \frac{U_o^2}{c_{p1}(T_{II} - T_I)}$ is the Eckert number, $\Pr = \frac{\mu_1 c_{p1}}{k_1}$ is the Prandtl number and $n_k = \frac{k_2}{k_1}$ is the thermal conductivity ratio.

In the nondimensional form, the boundary conditions for temperature and heat flux at the walls and interface become:

(i) At the lower and upper plate boundaries the temperatures are, respectively,

$$\theta_1 = 0 \quad \text{at } y = -1 \quad \text{and} \quad \theta_2 = 1 \quad \text{at } y = 1 \tag{17}$$

(ii) At the fluid interface temperature (θ) and heat flux ($\bar{\mathbf{h}}$) are continuous:

$$\theta_1 = \theta_2 \quad \text{and} \quad \frac{d\theta_1}{dy} = n_k \frac{d\theta_2}{dy} \quad \text{at } y = 0 \tag{18}$$

The solutions of Eqs. (15) and (16) with boundary and interface conditions are solved analytically. The solution involves four constants c_{15}, c_{16}, c_{25}, and c_{26} and these are found from the four boundary conditions (Eqs. (17) and (18)) and are obtained using Mathematica. Since they are lengthy they are not shown here.

Nusselt number

Heat transfer coefficient at the walls is given by Fourier's law of heat conduction $\overline{\mathbf{h}} = -k\nabla T$. In non-dimensional form this represents Nusselt number $Nu = -\left.\frac{d\theta}{dy}\right]_{y=\pm 1}$. This is studied only at the walls of the channel.

4. Second Law Analysis

Once the velocity and temperature profiles are obtained, one can determine the entropy generation distribution in a flow channel.

4.1 The volumetric entropy generation

It is assumed that each of the couple stress fluid has constant physical properties (ρ_i, μ_i, k_i, cp_i) and is flowing in the channel subjected to constant wall temperatures on each plate. If we take an infinitesimal fluid element in each zone and assume that the element is an open thermodynamic system subjected to mass fluxes, energy transfer and entropy transfer interactions through a fixed control surface, the volumetric rate of entropy generation for couple stress fluid is given as

$$\begin{aligned}\left(S_i\right)_G &= \underbrace{\left(S_i\right)_{\text{G, heat transfer}}}_{\geq 0} + \underbrace{\left(S_i\right)_{\text{G, viscous dissipation}}}_{\geq 0} + \underbrace{\left(\mathrm{S_i}\right)_{\text{G, Joule dissipation}}}_{\geq 0} \\ &= \frac{k}{T_o^2}\left[\nabla T\right]^2 + \frac{1}{T_o}\Phi + \frac{1}{T_o}\frac{\bar{J}^2}{\sigma}.\end{aligned}$$

For this study, the volumetric rate of entropy generation reduces to

$$(S_i)_G = \frac{k_i}{T_o^2}\left(\frac{\partial T_i}{\partial Y}\right)^2 + \frac{\mu_i}{T_o}\left(\frac{\partial U_i}{\partial Y}\right)^2 + \frac{\eta_i}{T_o}\left(\frac{\partial^2 u_i}{\partial Y^2}\right)^2 + \frac{\sigma_i}{T_o}H_o^2\,U_i^2, \tag{19}$$

where the value of i can be either 1 or 2 that represents fluid I or fluid II, respectively. On the right hand side of Eq. (19), the first term represents the entropy generation rate due to heat transfer irreversibility, the second and third terms are due to fluid friction irreversibility, and the last term is due to magnetic effect in the form of Joule dissipation irreversibility.

4.2 The characteristic entropy generation rate

The characteristic entropy generation rate $S_{G,C}$ is defined as,

$$S_{G,C} = \left[\frac{\bar{\mathbf{h}}_1^2}{k_1 T_o^2}\right] = \left[\frac{k_1\left(\Delta T\right)^2}{h^2 T_o^2}\right] \tag{20}$$

In the above equation, $\bar{\mathbf{h}}_1$ is the heat flux in zone I, T_o is the average, characteristic, absolute reference temperature of the medium, ΔT is the temperature difference and h is the half transverse distance of the channel.

4.3 The entropy generation number

According to Bejan [2], the dimensionless form of entropy generation is the entropy generation number (Ns) and which is, by definition, equal to the ratio of the actual generation rate to a characteristic entropy transfer rate. The entropy generation number for each fluid with dimensionless variables are given by

$$Ns_1 = \frac{(S_1)_G}{s_{G,C}} = \left(\frac{d\theta_1}{dy}\right)^2 + \left(\frac{Br}{\Omega}\right)\left[\left(\frac{du_1}{dy}\right)^2 + \frac{1}{s_1}\left(\frac{d^2u_1}{dy^2}\right)^2 + Ha^2u_1^2\right] \tag{21}$$

$$Ns_2 = \frac{(S_2)_G}{s_{G,C}} = n_k\left(\frac{d\theta_2}{dy}\right)^2 + n_\mu\left(\frac{Br}{\Omega}\right)\left[\left(\frac{du_2}{dy}\right)^2 + \frac{1}{s_2}\left(\frac{d^2u_2}{dy^2}\right)^2 + n_\sigma\, Ha^2u_2^2\right], \tag{22}$$

where $Br = (\frac{\mu_1 U_o^2}{k_1 \Delta T})$ is the Brinkman number, which determines the importance of viscous dissipation because of the fluid frictions relative to the conduction heat flow resulting from the impressed temperature difference and $\Omega = (\frac{\Delta T}{T_o})$ is the dimensionless temperature difference.

It is desirable to consider the Ek and Pr in a group that is called the Brinkman number (Br = Ek Pr) for evaluating the relative importance of the energy due to viscous dissipation to the energy because of heat conduction. It was reported that Br is much less than unity for many engineering processes [5].

4.4 The viscous dissipation parameter or Group parameter

The viscous dissipation parameter is an important dimensionless number for the irreversibility analysis. It determines the relative importance of the viscous effects for the entropy generation and it is equal to the ratio of the Brinkman number to the dimensionless temperature difference, i.e., (Br/Ω).

Equations (21), (22) can be expressed alternatively as follows:

$$Ns_i = Ny_i + Nf_i + Nm_i \quad (i = 1, 2), \tag{23}$$

where the first term (Ny_i) denotes the entropy generation due to heat transfer conduction in the transverse direction, the second term (Nf_i) represents the entropy generation due to the viscous dissipation effect that results from the fluid frictions, and the last term (Nm_i) is the entropy generation due to the magnetic field.

4.5 Fluid friction versus heat transfer irreversibility

The convective heat transfer processes are analyzed by the second law of thermodynamics namely entropy generation due to the irreversibility of the processes. As stated earlier, there exists a direct proportionality between irreversibility (quantified in the entropy generated) and the amount of useful and available work lost in the process. In convective heat transfer both fluid frictions and heat transfer make contributions to the rate of entropy generation. Entropy generation number (Ns) is good for generating entropy generation profiles but fails to give any idea about the relative importance of friction and heat transfer effects. The domination of the irreversibility mechanisms is physically important since the entropy generation number is unable to overcome this problem. Two alternate parameters, irreversibility distribution ratio (ϕ) and Bejan number (Be) are introduced for this purpose and they are gaining increasing popularity among researchers studying the second law.

4.5.1 The Irreversibility ratio

The idea of irreversibility distribution ratio ϕ can enhance the understanding of the irreversibility's associated with the heat transfer and the fluid friction. It is defined as the ratio of entropy generation due to fluid frictions (*Nf*) to heat transfer and magnetic field in the transverse direction (Ny), i.e.,

$$\phi = \frac{S_{\mathrm{G,\,fluid\ friction}} + S_{\mathrm{G,\,magnetic\ field}}}{S_{\mathrm{G,\,heat\ transfer}}} = \left(\frac{Nf + Nm}{Ny}\right).$$

Here ϕ can be interpreted as follows: If $0 \leq \Phi < 1$, then ϕ indicates that heat transfer irreversibility dominates and if $\phi > 1$ the irreversibility is dominated by the combined effects of fluid friction and magnetic fields. When $\phi = 1$, contribution of heat transfer to entropy generation is equal to the sum of fluid friction and magnetic field.

4.5.2 The Bejan number

An alternative irreversibility distribution parameter, called the Bejan number Be, was defined by Paoletti and colleagues [34], as the ratio of entropy generation due to heat transfer to the total entropy generation and it is given by

$$\begin{aligned}\mathrm{Be} &= \frac{\text{heat transfer irreversibilty}}{\text{heat transfer irreversibilty} + \text{fluid friction irreversibility} + \text{Joule dissipation irreversibility}} \\ &= \frac{Ny}{Ns} = \frac{Ny}{Ny + Nf + Nm} = \frac{1}{1+\phi}\end{aligned} \tag{24}$$

This is employed to understand the entropy generation mechanisms as proposed by Bejan [2, 5].

The value of Be $\rightarrow$ 1 indicates that the heat transfer irreversibility dominates over fluid friction, and this corresponds to the case of $\phi \rightarrow 0$. On the other hand, Be $\rightarrow$ 0 indicates that the fluid friction and Joule dissipation irreversibility dominate entropy generation. This corresponds to $\phi \rightarrow \infty$. It is obvious that Be = 0.5 is the case in which the contribution of the heat transfer

irreversibility is equal to the sum of the fluid friction and Joule dissipation and this corresponds to the case of $\phi = 1$.

4.6 Importance of second law

By the first law of thermodynamics, we can find the temperature distributions of fluids within the channel and also heat transfer coefficients at the plates. But this law will not give any information regarding the relative effects of viscosity and heat convection for entropy generation. The second law states that entropy is always positive. The law is also stated in the form of inequality of entropy generation. It can be noted that the second law analysis makes it possible to compare many different interactions in a system or process, and to identify the major sources of exergy destructions/losses. This enables us to identify the exact region where the entropy generation rate is more in the entire fluid regime. This study is facilitated through the entropy generation number (Ns) introduced by Bejan [2, 5]. The relative effects of dissipation energy and heat transfer can be studied through the Bejan number Be (Paoletti and colleagues [34]).

5. Results and Discussion

The first and second laws of thermodynamics for the flow of two immiscible couple stress fluids in the presence of a constant applied magnetic field are obtained and reported in the previous section. The parameters which influence the flow, heat transfer and entropy generation rate inside the channel are the couple stress parameter s_2, Reynolds number Re, Hartmann number Ha and viscous dissipation (or group) parameter (Br/Ω). The variations of velocity, temperature, entropy generation number and Bejan number for different values of these parameters are shown through figures.

5.1 Flow field

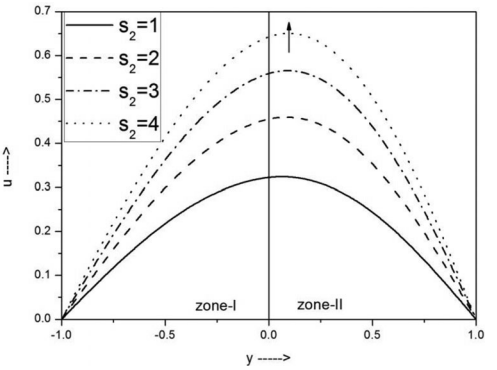

Fig. 2. Effect of couple stress parameter $s_2$on velocity u for B $= -1.2$, Ha $= 0.1$, $n_\sigma = 0.8$, $n_\eta = 0.8$, $n_\mu = 0.8$, Re $= 2$, $s_1 = 2$.

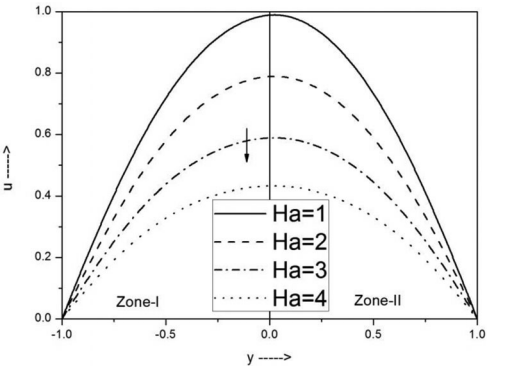

Fig. 3. Effect of Hartmann number Ha on velocity u for B $= -1.5$, $n_\sigma = 0.6$, $n_\eta = 0.8$, $n_\mu = 0.6$, Re $= 2$, $s_1 = 2$, $s_2 = 2$.

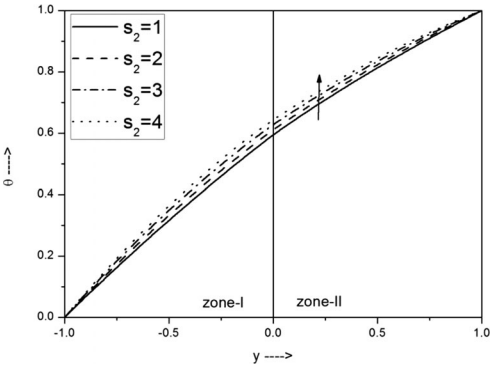

Fig. 4. Effect of couple stress parameter s_2 on temperature θ for B $= -0.4$, Br $= 2$, Ha $= 0.2$, $n_\sigma = 0.8$, $n_\eta = 0.8$, $n_\mu = 0.5$, $n_k = 1.1$, Re $= 1.8$, $s_1 = 2$.

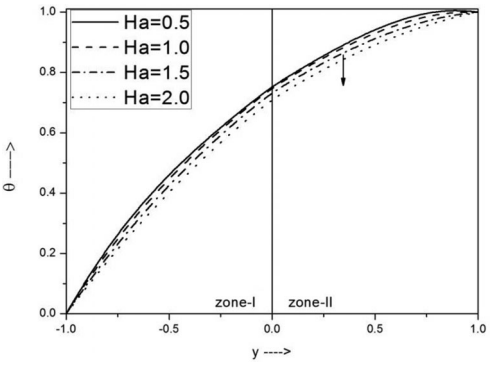

Fig. 5. Effect of Hartmann number Ha on temperature θ for B $= -1.2$, Br $= 0.8$, $n_\sigma = 0.9$, $n_\eta = 0.8$, $n_\mu = 0.9$, $n_k = 1.2$, Re $= 1.5$, $s_1 = 7$, $s_2 = 7$.

5.2 Thermal field

The effect of the couple stress parameter s_2 on the velocity field is shown in Figure 2. It is seen that as s_2 increases, the velocity increases in both zones of the channel. As $s_i \to \infty$ (i = 1,2) we get the case of a Newtonian fluid. Hence from Figure 2 we conclude that velocity of the viscous fluid is more than that of the couple stress fluid. The effect of the Hartmann number Ha on the velocity field is shown in Figure 3. It is seen that as the Hartmann number Ha increases, the velocity decreases in the channel. From Eq. (4), it can be observed that the magnetic field as a body force opposes the flow and hence the decrease in velocity is a retarding influence on the flow. Hence we conclude that the imposed magnetic field has a retarding influence on the flow field.

The effect of the couple stress parameter s_2 on the temperature field is shown in Figure 4. It is seen that as s_2 increases, the temperature increases in both zones of the channel. Since velocity is increased, the temperature due to dissipation of energy (depending on velocity) also increases. The effect of the Hartmann number Ha on the temperature distribution is shown in Figure 5. As the Hartmann number Ha increases, temperature decreases. This may be due to the fact that as Ha increases, velocity decreases, hence dissipation of energy decreases and this in turn leads to the decrease in temperature.

5.3 Heat transfer

Figure 6 presents the effect of Reynolds number Re on the Nusselt number Nu as a function of Brinkman number Br. It is observed that as the Reynolds number Re increases the Nusselt number Nu increases. Figure 7 shows the effect of Hartmann number Ha on the Nusselt number Nu as a function of Brinkman number Br. It is observed that as the Hartmann number Ha increases, the Nusselt number Nu decreases.

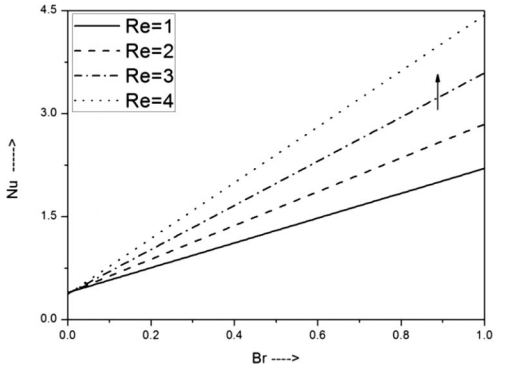

Fig. 6. Effect of Reynolds number Re on Nusselt number as a function of Br for $B = -2$, $Ha = 0.1$, $n_\sigma = 0.8$, $n_\eta = 0.9$, $n_\mu = 0.6$, $n_k = 0.7$, $s_1 = 2$, $s_2 = 2$.

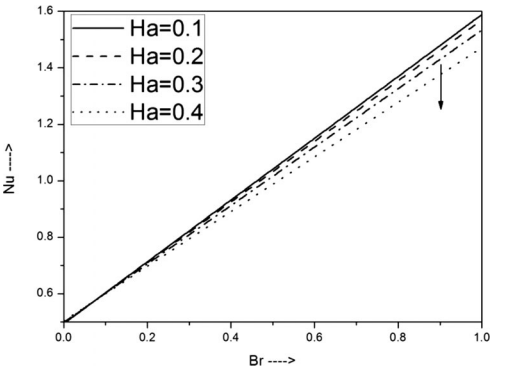

Fig. 7. Effect of Hartmann number Ha on Nusselt number as a function of Br for $B = -1.5$, $n_\sigma = 0.9$, $n_\eta = 0.9$, $n_\mu = 0.9$, $n_k = 0.9$, $Re = 2$, $s_1 = 2$, $s_2 = 2$.

5.4. Entropy generation and Heat transfer irreversibility

Figure 8 describes the effect of couple stress parameter s_2 on entropy generation number Ns. As s_2 increases, entropy generation rate Ns increases near the walls in both zones of the channel and decreases at the interface. Entropy generation rate depends on velocity and temperature gradients (Eqs. (21)) and (22) and they increase as s_2 increases. Hence entropy generation rate increases at the boundaries (walls). Figure 9 shows the effect of Reynolds number Re on entropy generation number Ns. As Re increases, Ns increases. Figure 10 displays the variation of entropy generation number Ns as a function of y at different values of Hartmann number Ha. It is observed that as Ha increases, Ns decreases drastically near the plates and has a negligibly small effect at the interface. From Figures 8 and 9, it is observed that the entropy generation near the plates

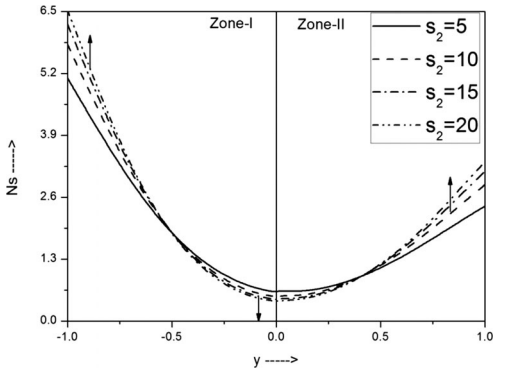

Fig. 8. Effect of couple stress parameter s_2 on entropy generation number Ns for $B = 3$, $Br = 0.5$, $Ha = 0.5$, $n_\sigma = 0.6$, $n_\eta = 0.6$, $n_\mu = 0.4$, $n_k = 0.7$, $Re = 2.2$, $s_1 = 10$, $\Omega = 1$.

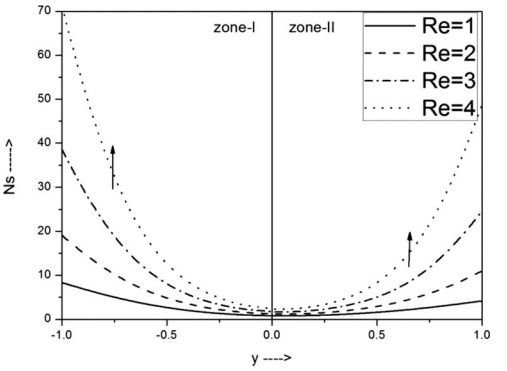

Fig. 9. Effect of Reynolds number Re on entropy generation number Ns for $B = -1.2$, $Br = 0.3$, $Ha = 0.1$, $n_\sigma = 0.8$, $n_\eta = 0.9$, $n_\mu = 0.8$, $n_k = 0.9$, $s_1 = 10$, $s_2 = 10$, $\Omega = 1$.

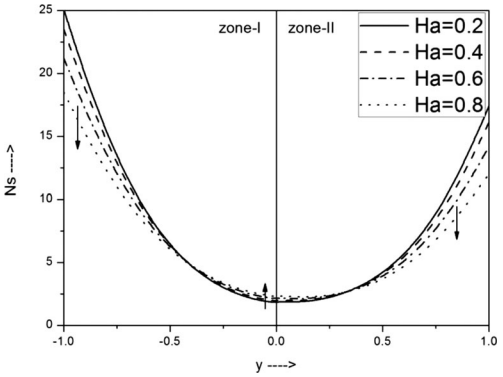

Fig. 10. Effect of Hartmann number Ha on entropy generation number Ns for B $= -1.8$, Br $= 1.2$, $n_\sigma = 0.8$, $n_\eta = 0.8$, $n_\mu = 0.8$, $n_k = 1$, Re $= 2$, $s_1 = 8$, $s_2 = 8$, $\Omega = 1$.

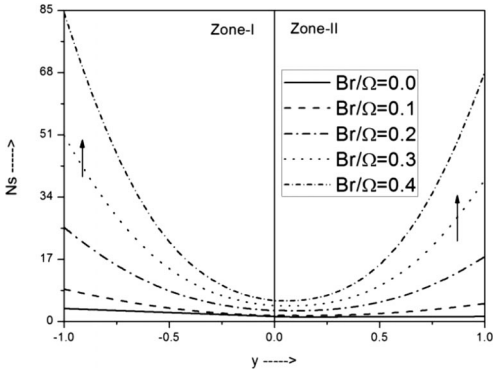

Fig. 11. Effect of viscous dissipation parameter (Br$/\Omega$) on entropy generation number Ns for B $= -2$, Ha $= 0.1$, $n_\sigma = 0.8$, $n_\eta = 0.8$, $n_\mu = 0.8$, $n_k = 1.2$, Re $= 4$, $s_1 = 4$, $s_s = 4$.

increases more rapidly in Zone I than in the Zone II. This is due to the fact that in Zone I fluid is more viscous.

From Figure 11, we observe that as the viscous dissipation parameter (Br/Ω) increases, the entropy generation number Ns increases. The greater the viscosity of the fluid, the greater the entropy generation rate. It is observed that Ns $\cong 0$ at the interface of the channel. This implies that at the interface, entropy generation is minimum i.e., exergy is maximum (available energy) and hence the dissipation of energy is almost zero and the thermal process is almost reversible there. When (Br/Ω) $\rightarrow 0$, the entropy generation number Ns $\rightarrow 1$ and becomes independent of the transverse distance. This is an ideal case which corresponds to the energy due to only the heat conduction and the effect of viscous dissipation disappears. There is a lowest point of the entropy generation rate at each specified value of the viscous dissipation parameter and it occurs near the interface. The profiles indicate that at the interface $y = 0$, the entropy generation rate is minimum and hence the available energy in the transverse direction is maximum.

Figure 12 depicts the effect of couple stress parameter s_2 on Bejan number Be. As s_2 increases, Bejan number decreases near the walls and increases at the interface. This indicates that irreversibility is almost zero at the interface. Figure 13 illustrates the effect of Reynolds number Re on Bejan number Be. As Re increases, Be decreases. The variation of Be near the plates is more than that at the interface. This indicates that frictional forces are increasing rapidly near the walls. Figure 14 predicts the variation of Bejan number Be as a function of y at different values of Hartmann number Ha. As Ha increases, Be increases drastically near the plates and decreases at the interface. As the Hartmann number increases, the curve for the Bejan number becomes flat for a considerable distance in the middle of the channel. This shows that magnetic effect decreases friction at the walls but increases the entropy generation rate at the interface. This is a significant observation that can be made from the present study in view of its practical applicability.

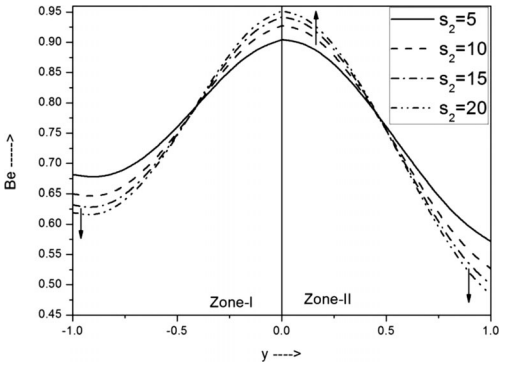

Fig. 12. Effect of couple stress parameter s_2 on Bejan number Be for B $= -0.1$, Br $=$ 5,Ha $= 0.1$, $n_\sigma = 0.9$, $n_\eta = 0.9$, $n_\mu = 0.9$, $n_k = 0.9$, Re $= 2.5$, $s_1 = 5$, $\Omega = 1$.

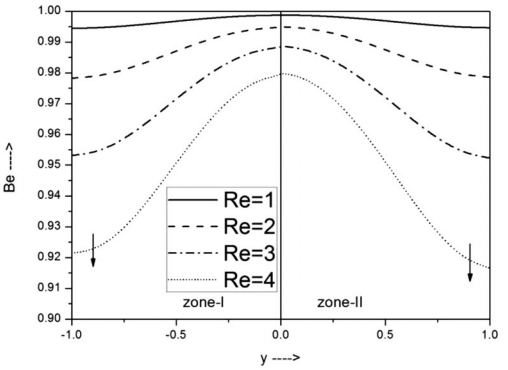

Fig. 13. Effect of Reynolds number Re on Bejan number Be for $B = -0.1$, Br $=$ 0.1,Ha $= 0.1$, $n_\sigma = 0.8$, $n_\eta = 0.8$, $n_\mu = 0.8$, $n_k = 0.8$, $s_1 = 8$, $s_2 = 8$, $\Omega = 1$.

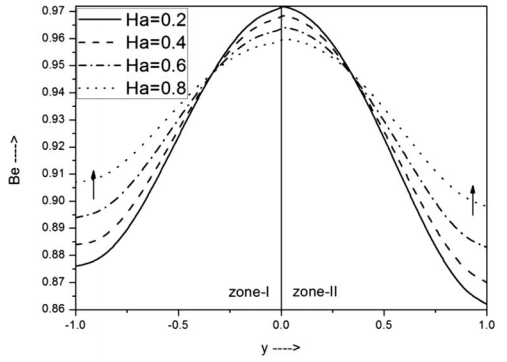

Fig. 14. Effect of Hartmann number Ha on Bejan number Be forB $= -0.5$, Br $= 0.1$, $n_\eta = 0.8$, $n_\mu = 0.8$, $n_\sigma = 0.8$, $n_k = 0.8$, Re $= 2$, $s_1 = 10$, $s_2 = 10$, $\Omega = 1$

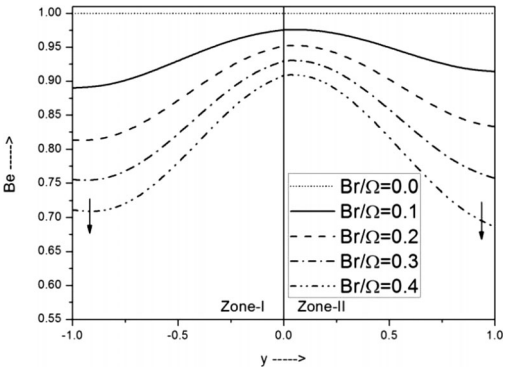

Fig. 15. Effect of viscous dissipation parameter (Br$/\Omega$) on Bejan number Be for $B = -0.1$, $Ha = 0.1$, $n_\eta = 0.8$, $n_\mu = 0.9$, $n_k = 0.8$, $n_\sigma = 0.8$, Re $= 8$, $s_1 = 8$, $s_2 = 8$.

From Figure 15, we observe that as the viscous dissipation parameter (Br/Ω) increases, Bejan number Be decreases. This shows that the Bejan number is maximum at the interface of the channel and decreases as we move towards the channel walls in either direction. We again observe that for (Br/Ω) $= 0$, Be is equal to its maximum theoretical value (Be $= 1$), i.e., the fluid friction effect provides no contribution to the entropy generation. For all other values of (Br/Ω), the Bejan number has a maximum value close to the central line of the channel and then decreases near the walls.

6. Conclusions

An analytical study of the first and second laws of thermodynamics is presented to investigate the effects of viscous dissipation and magnetic force in two immiscible couple stress fluids

between two parallel plates. The velocity and temperature profiles are obtained analytically and used to compute the entropy generation number Ns and Bejan number Be. Bejan number is used to find relative effects of frictional forces and heat conduction. The effects of the viscous dissipation parameter (Br/Ω) and Hartmann number Ha on the entropy generation number Ns and Bejan number Be are studied analytically. The computational results are presented through figures. It is observed that

1. The entropy generation number Ns is dependent on the velocity and the temperature distributions. At the value of $(Br/\Omega) = 0$, the entropy generation distribution is observed to be independent of the transverse distance. The entropy generation increases with increasing the viscous dissipation parameter (Br/Ω).

2. The values of Ns near the plates are more than what they are at the interface, indicating that friction due to surface on the fluids increases entropy generation rate.

3. The values of Ns in Zone I are more than what they are in the Zone II near the plates. This indicates that greater the viscosity of the fluid, the greater is the entropy generation rate.

4. The Bejan number is maximum and the irreversibility ratio is minimum at the interface of the channel. This indicates that the amount of exergy (available energy) is maximum and irreversibility is minimum at the interface.

5. Increasing the value of Ha (i.e., magnetic force) has a tendency to retard the fluid motion inside the channel and to decrease the friction at the walls. This allows us to conclude that couple stress fluids can be used as good lubricants.

6. The plates act as strong sources of irreversibility.

Acknowledgments

The authors would like to express thanks to the reviewers for their valuable comments and suggestions for the improvement of the paper.

Literature Cited

1. Bejan A. Second law analysis in heat transfer and thermal design. Adv Heat Transf 1982;15:1–58.
2. Bejan A. Entropy generation minimization, CRC Press, Boca Raton, NY, 1996.
3. Bejan A. Entropy generation through heat and fluid flow, Wiley, New York, 1982.
4. Bejan A. Advanced engineering thermodynamics, 2nd ed., Wiley, New York, 1997.
5. Bejan A. A study of entropy generation in fundamental convective heat transfer. J Heat Transf 1979;101:718–725.
6. Bejan A. Second law analysis in heat transfer. Energy 1980;5:720–732.
7. San JY, Worek WM, Lavan Z. Entropy generation in convective heat transfer and isothermal convective mass transfer. J Heat Transf 1987;109:647–652.

8. Demirel Y & Kahraman R. Thermodynamic analysis of convective heat transfer in an annular packed bed. Int J Heat Fluid Flow 2000;21:442–448.
9. Delavar MA, Hedayatpour M. Forced convection and entropy generation inside a channel with a heat-generating porous block. Heat Transf Asian Res 2012;41(7):580–600.
10. Hooman K, Ejlali A, Hooman F. Entropy generation analysis of thermally developing forced convection in fluid-saturated porous medium. Appl Math Mech 2008;29(2):229–237.
11. Bird RB, Stewart WE, Lightfoot EN. Transport phenomena, John Wiley and Sons, Inc, New York, 1960.
12. Chaturani P, Ponnalagar Samy R. A study of non-Newtonian aspects of blood flow through stenosed arteries and its applications in arterial diseases. J Biology 1985;22(6):521–531.
13. Ramchandra Rao A, Srinivasan Usha. Peristaltic transport of two immiscible viscous fluids in a circular tube. J Fluid Mech 1995;298:271–285.
14. Bakhtiyarov SI, Siginer DA. A note on the laminar core-annular flow of two immiscible fluids in a horizontal tube. Proceed. Int. Symposium on liquid-liquid two phase flow and transport phenomena, Begell house, Inc., Santa Barbara, 1997, 107–111.
15. Prathap Kumar J, Umavathi JC, Basavaraj M Biradar. Mixed convective flow of immiscible viscous fluids in a vertical channel. Heat Transf Asian Res 2011;40(1): 1–25.
16. Chamkha AJ. Flow of two immiscible fluids in porous and nonporous channels. J Fluids Eng 2000;122:117–124.
17. Attia HA, Kotb NA. MHD flow between two with heat transfer parallel plates. Acta Mechanica 1996;117:215–220.
18. Ashraf M, Wehgal AR. MHD flow and heat transfer of micropolar fluid between two porous disks. Appl Math Mech 2012;33(1):51–64.
19. Alpher RA. Heat transfer in magnetohydrodynamic flow between parallel plates. Int. J Heat Mass Transf 1961;3(2):108–112.
20. Nikodijevic D, Milenkovic D, Stamenkovic Z. MHD Couette two-fluid flow and heat transfer in presence of uniform inclined magnetic field. Heat Mass Transf 2011;47(12):1525–1535.
21. Damseh RA, Al-Odat MQ, Al-Nimr MA. Entropy generation during fluid flow in a channel under the effect of transverse magnetic field. Heat Mass Transf 2008;44(8):897–904.
22. Mahian O, Mahmud S, Pop I. Analysis of first and second laws of thermodynamics between two isothermal cylinders with relative rotation in the presence of MHD flow. Int J Heat Mass Transf 2012;55(17-18):4808–4816.
23. Kiyasatfar M, Pourmahmoud N, Golzan MM, Mirzaee I. Thermal behavior and entropy generation rate analysis of a viscous flow in MHD micropumps. J Mech Sci Technol 2012;26(6):1949–1955.
24. Chin-Chia Liu, Cheng-Ying Lo. Numerical analysis of entropy generation in mixed-convection MHD flow in vertical channel. Int Comm Heat Mass Transf 2012;39(9):1354–1359.
25. Kamisli F, Oztop HF. Second law analysis of the 2D laminar flow of two-immiscible, incompressible viscous fluids in a channel. Heat Mass Transf 2008;44(6):751–761.
26. Stokes VK. Couple stresses in fluid. Phys. Fluids 1966;9(9):1709–1715.
27. Stokes VK. Theories of fluids with microstructures, Springer, New York, 1984.
28. Soundalgekar VM, Aranake RN. Effects of couple stresses on MHD Couette flow. Nuclear Eng Design 1978;49(3):197–203.
29. Srivastava LM. Peristaltic transport of a couple stress fluid. Rheol Acta 1986;25:638–641.
30. Shehawey EFE, Mekheimer KS. Couple stresses in peristaltic transport of fluids. J Phys D Appl Phys 1994;27:1163–1170.
31. Naduvinamani NB, Hiremath PS, Gurubasavaraj G. Surface roughness effects in a short porous journal bearing with couple stress fluid. Fluid Dyn Res 2002;31:333–354.

32. Naduvinamani NB, Hanumagowda BN, Fathima ST. Combined effects of MHD and surface roughness on couple-stress squeeze film lubrication between porous circular stepped plates. Tribol Int J 2012;56:19–29.
33. Muthuraj R, Srinivas S, Selvi RK. Heat and mass transfer effects on MHD flow of a couple stress fluid in a horizontal wavy channel with viscous dissipation and porous medium. Heat Transf Asian Res 2013;42(5):403–421.
34. Paoletti S, Rispoli F, Sciubba E. Calculation exergetic loses in compact heat exchanger passages. ASME AES 1989;10:21–29.

□♦ ♦ ♦□